EXPERIMENTAL INVESTIGATION OF LAMINAR MIXED CONVECTION IN AN INCLINED ANNULUS

Prof. Dr. Khalid A. Ismael
Mech. Engr. Dept.
University of Technology
Baghdad-Iraq

Asst. Prof. Dr. Ihsan Y. Hussain
Mech. Engr. Dept.
College of Engr.
University of Baghdad
Baghdad-Iraq

Asst. Lecturer Akeel A. Mohammed
Mech. Engr. Dept.
University of Technology
Baghdad-Iraq

ABSTRACT

Experiments were carried out to study the local and average heat transfer by mixed convection to a simultaneously developing air flow in a horizontal , inclined, and vertical concentric cylindrical annulus. The experimental setup consists of an annulus has a radius ratio of 0.555 and inner cylinder with a heated length 1.2m subjected to the constant heat flux while the outer cylinder is subjected to the ambient temperature. The investigation covers Reynolds number range from 154 to 845, heat flux varied from 96 W/m^2 to 845 W/m^2, and annulus angles of inclinations α =0° (horizontal), 40°, 70°, and 90° (vertical). Results demonstrate the temperature variation along the inner cylinder surface and the local Nusselt number Nu_z variation with the dimensionless axial distance , for all angles of inclinations which shows an increase in the Nu_z values as the heat flux increases and as the angle of the inclination moves from the vertical to the horizontal position.

الخلاصة

أجريتْ تجارب عملية لدراسة انتقال الحرارة الموقعي و المعدّل بالحمل المختلط لجريان الهواء المشكّل تراكبياً (أي تزامن التشكيل الحراري مع التشكيل الهيدروديناميكي) بتجويف حلقي بين اسطوانتين متحدي المركز، نسبة نصف القطر لهما تعادل 0.555 و بطول 1.2 m ، بالوضع الأفقي، المائل، و العمودي. سخنت الاسطوانة الداخلية تحت فيض حراري ثابت ، بينما عرّضت الاسطوانة الخارجية إلى درجة حرارة الجو. يتراوح معدّل رقم رينولدز Re في هذا البحث من 154 إلى 845 أما الفيض الحراري فيتغير من 96 W/m^2 إلى 860 W/m^2 ، و زوايا ميل التجويف الحلقي هي 0° (أفقي)، 40° ، 70° ، 90° (عمودي). . وضحت النتائج العملية تغير درجة حرارة الأسطوانة الداخلية مع الاتجاه الطولي و كذلك تغير رقم نسلت الموقعي مع المسافة المحورية الغير بعدية ، حيث أظهرت النتائج زيادة رقم نسلت مع زيادة الفيض الحراري و مع انحراف زاوية الميل من الوضع العمودي إلى الوضع الأفقي.

KEY WORDS
Heat Transfer, Mixed Convection, Concentric Annulus

INTRODUCTION

Laminar flow heat transfer in annuli is encountered in a wide variety of engineering situations, including the barrel- type expitaxial reactor (chemical vapor deposition reactor) in the semi

conductor manufacturing industry (Hanzwa 1986), heat exchangers designed for viscous liquids in chemical process and food industries (Hessami 1987), the cooling of electrical cables, the collection of solar energy (Ciampi 1987), etc. In many of these applications, flow through the annular passage is characterized by small Reynolds numbers for which buoyancy effects may be significant. Even though such applications are now being used widely, there is a lack of understanding of many details of laminar flow and heat transfer physics concepts. The difficulties with laminar flows are associated with the fact that fluids which in practice are in this flow regime usually have properties which are strongly dependent on temperature. As a result, to cover this lack, the present study is motivated and concerned with the experimental investigation of laminar mixed convection in the thermal and hydrodynamic entrance region of concentric annulus with uniformly heated inner cylinder, and outer cylinder subjected to ambient.

Many experimental and theoretical investigations have been conducted to study the effect of free convection on laminar flow inside horizontal, inclined, and vertical annulus.- (Lundberg, et-al 1962). studied experimentally and theoretically the mixed convection of simultaneously developing laminar upward air flow in a vertical annulus. The experimental study included four annulus radius ratios (0.132, 0.25, 0.375, and 0.5).The thermal condition of the inner wall was isothermal and the outer wall was adiabatic, while Re varied from 800 to 1500. Variation of the inner surface temperature and the heat transfer coefficient along annulus were depicted. While the theoretical study included evaluation of the four fundamental solutions in the thermal energy regions by solution of the eigen value problem.

(Hanzawa, ét-al 1986), performed experiments to study the mixed convection of upward gas flow in a vertical annulus of radius ratio range from 0.39 to 0.63 and hydraulic diameter to heating section length range from 0.34 to 1.4 . A part of the inner tube was isothermally heated while the outer tube was kept adiabatic. Study covered Gr range from 1.5×10^5 to 2.6×10^8 , Re range from 20 to 100. The effects of operating conditions on the temperature profiles, flow pattern and heat transfer coefficient were investigated. (Falah & Yaseen 1993) performed experiments to study the local and average heat transfer by mixed convection to a simultaneously developing upward air flow in a vertical , inclined and horizontal concentric cylindrical annulus with a radius ratio of 0.41 and the inner cylinder with a heated length of 0.85 m was subjected to the ambient temperature. The investigation has covered Re range from 300 to 1200, heat flux varied from 90 W/m^2 to 680 W/m^2 and annulus angle of inclination 0°(vertical), 30°, 45°, 60° , and 90° (horizontal). The results show that the heat transfer process improves as the angle of inclination deviates from the vertical to the horizontal position.

EXPERIMENTAL APPARATUS

An open air circuit was used which included a compressor (B) , orifice plate section (C), settling chamber (D), test section and a flexible hose (E). The air which is driven by compressor can be regulated accurately by using two control valves, as shown diagrammatically in **Fig. (1)**. The air induced by the compressor , enters the orifice pipe section (Standard British Unit) and then settling chamber through a flexible hose (E). The settling chamber was carefully designed to reduce the flow fluctuation and to get a uniform flow at the test section entrance by using flow straightener (G). The air then passed through 1.2 m long test section. A symmetric flow and a uniform velocity profile produced by a well design Teflon bell mouth (H) which is fitted at the annulus outer aluminum cylinder (I) and bolted inside the settling chamber (D). The inlet air temperature was measured by one thermocouple (J) located in the settling chamber (D) while the outlet bulk air temperature was measured by three thermocouples (Z) located in the test section exit. The local bulk air temperature was calculated by using a straight line interpolation between the measured inlet and outlet bulk air temperature.

The test section consisted of 4 mm wall thickness, 50 mm outside diameter and 1.2 m long aluminum cylinder (K) located centrally in 5 mm thickness , 90 mm inside diameter and 1.2 m long

aluminum cylinder, by fitting it at the test section inlet with the 20 mm inside diameter , 50 mm outside diameter and 15 mm long Teflon tube (N) and at the test section exit with the teflon piece (M). A ring (P) is used to hold and support the aluminum cylinder (K) with the teflon piece (N) centrally inside the settling chamber by adjustable screws (Q). The teflon was chosen because of its low thermal conductivity in order to reduce the heat loss from the aluminum cylinder ends.

The inner cylinder was heated electrically using an electrical heater which consists of a nickel-chrome wire ®, wound as a coil spirals around solid teflon tube and is covered by a 2 mm thickness asbestos layer , and the space between the asbestos and the inner cylinder wall is fitted with a fine grade sand to avoid heat convection in it and to smooth out any irregularities in the heat flux. The hole apparatus is designed with a view to obtain a good concentricity of the core cylinder and the containing cylinder. The temperature of the outside surface of the inner cylinder was measured by seventeen asbestos sheath alumel-chromel (type K) thermocouples , arranged along the cylinder , the measuring heads of the thermocouples were made by fusing together the ends of two wires.

The thermocouples were fixed by drilling holes of 1.5 mm diameter in the cylinder wall and the ends of the holes chamfered by a 3 mm slug to locate the measuring junctions which were then fixed by a high temperature application Defcon adhesive . The excess adhesive was removed and the cylinder outer surface was cleaned carefully by fine grinding paper. All the thermocouples wires and heater terminals were taken out the test section through both teflon pieces (N,M) .

On the other hand , there were twelve thermocouples placed in three sections along the inner cylinder of the annulus (at z=1 cm, 53 cm, 108 cm) , four for each section arranged at angle (ϕ=0°, 90°, 180°, 270°) around the inner cylinder. Other ten thermocouples were (type K) used to measure the inner surface temperature of the annulus outer cylinder (I). Thermocouples positions at the outer surface were located and then a 2 mm deep pits were drilled in which the thermocouples were fixed by Defcon adhesive. All thermocouples were used with leads , the thermocouple with lead and without lead were calibrated against the melting point of ice made from distilled water and the boiling points of several pure chemical substances. To determine the heat loss from the test section ends, two thermocouples were fixed in each teflon piece. The distance between these thermocouple was 12 mm. Knowing the thermal conductivity of the teflon , the ends condition could thus be calculated.

EXPERIMENTAL PROCEDURE

To carry out an experiment the following procedure was followed:

1- The inclination angle of the annulus was adjusted as required.

2- The compressor was then switched on to circulate the air , through the open loop. A regulating valves were used for adjusting the required mass flow rate.

3- The electrical heater was switched on and the heater input power then adjusted to give the required heat flux.

4- The apparatus was left at least three hours to establish steady state condition. The thermocouples readings were measured every half an hour by means of the digital electronic multimeter until the reading became constant , a final reading was recorded. The input power to the heater could be increased to cover another run in a shorter period of time and to obtain steady state conditions for next heat flux and same Reynolds number. Subsequent runs for other Reynolds number and annulus inclination angle ranges were performed in the same previous procedure.

5- During each test run , the following readings were recorded:

a- The angle of inclination of the annulus in degree.

b- The reading of the manometer (air flow rate) in mm H_2o.

c- The readings of the thermocouples in °C.

d- The heater current in amperes.

e- The heater voltage in volts.

DATA ANALYSIS

Simplified steps were used to analyze the heat transfer process for the air flow in an annulus where the inner cylinder was subjected to a uniform heat flux while the outer cylinder was subjected to the ambient temperature. The total input power supplied to the inner cylinder can be calculated:

$$Q_t = V'' \times I \qquad (1)$$

The convection and radiation heat transferred from the inner cylinder is :

$$Q_{cr} = Q_t - Q_{cond} \qquad (2)$$

where Q_{cond} is the conduction heat loss which was found experimentally equal to 3 % of the input power. The convection and radiation heat flux can be represented by:

$$q_{cr} = Q/A_1 \qquad (3)$$

where ($A_1 = 2\pi r_1 L$)

The convection heat flux , which is used to calculate the local heat transfer coefficient is obtained after deduce the radiation heat flux from q_{cr} value. The local radiation heat flux can be calculated as follows:

$$q_r = F_{1-2}\ \varepsilon\ \sigma\left[\left((t_s)_z + 273\right)^4 - \left(\overline{(t_{s2})_z} + 273\right)^4\right] \qquad (4)$$

where:

F_{1-2}= view factor between inner and outer cylinder ≈1

$(t_s)_z$ = local temperature of inner cylinder.

$\overline{(t_{s2})_z}$ = average temperature of outer cylinder.

ε = emissivity of the polished aluminum surface=0.09.

Hence the convection heat flux at any position is:

$$q = q_{cr} - q_r \qquad (5)$$

The local heat transfer coefficient can be obtained as:

$$h_z = \frac{q}{(t_s)_z - (t_b)_z} \qquad (6)$$

$(t_b)_z$ = Local bulk air temperature.

All the air properties were evaluated at the mean film air temperature (Keys 1966):

$$(t_f)_z = \frac{(t_s)_z + (t_b)_z}{2} \qquad (7)$$

t_f = Local mean film air temperature.

The local Nusselt number (Nu_z) then can be determine as:

$$Nu_z = \frac{h_z \quad D_h}{\kappa} \tag{8}$$

The average values of Nusselt number Nu_m can be calculated based on calculation of average inner surface temperature and average bulk air temperature as follows:

$$\overline{t_s} = \frac{1}{L} \int_{z=0}^{z=L} (t_s)_z \quad dz \tag{9}$$

$$\overline{t_b} = \frac{1}{L} \int_{z=0}^{z=L} (t_b)_z \quad dz \tag{10}$$

$$\overline{t_f} = \frac{\overline{t_z} + \overline{t_b}}{2} \tag{11}$$

$$Nu_m = \frac{q \quad D_h}{k(\overline{t_z} - \overline{t_b})} \tag{12}$$

The average values of the other parameters can be calculated as:

$$Re_m = \frac{\rho \quad u_i \quad D_h}{\mu} \tag{13}$$

$$Gr_m = \frac{g \quad \beta \quad D_h^3 \quad (\overline{t_z} - \overline{t_b})}{\nu^2} \tag{14}$$

$$Pr_m = \frac{\mu \quad C_p}{k} \tag{15}$$

$$Ra_m = Gr_m \cdot Pr_m \tag{16}$$

where:

$$\beta = 1/(273 + \overline{t_f})$$

$$u_i = \dot{m}/\rho A$$

$$A = \pi \left(r_2^2 - r_1^2\right)$$

All the air physical properties ρ, μ, ν, and k were evaluated at the average mean film temperature ($\overline{t_f}$).

EXPERIMENTAL RESULTS

Range of Experiments

A total of 46 test runs carried out to cover annulus inclination angles, horizontal (α=0°), inclined (α=40° and 70°) and vertical (α=90°). The range of heat flux 96 W/m^2 to 860 W/m^2 and Reynolds number varied from 154 to 845.

Temperature Variation

The temperature variation in the horizontal position is plotted for selected runs in **Figs. (2)** and **Fig. (3)**. The variation of the surface temperature along inner cylinder for different heat flux and for approximately Re=218 is shown in **Fig. (2)**. It is obvious that the surface temperature increases at the stage of entrance and attains a maximum point after which the surface temperature begins to decrease at high heat flux and be almost constant for very small heat flux. The rate of surface temperature rises at early stage is directly proportional to the wall heat flux. The point of maximum temperature seems to move toward the annulus entrance as the heat flux increases. This can be attributed to the increasing of the thermal boundary layer faster due to buoyancy effect as the heat flux increases at the same Reynolds number.

Fig. (3) shows the effect of Reynolds number variation on the inner cylinder surface temperature for heat flux (q=682 W/m^2). It can be noticed that, the increasing of Reynolds number reduces the surface temperature as heat flux kept constant and the surface temperature values at entrance and at the same axial distance seem to be closer to each other then diverges downstream. This can be attributed to poverty of natural convection at annulus entrance and high mixing cup downstream.

The variations of surface temperature along the axis of vertical annulus for different Reynolds number and heat flux equals to 265 W/m^2 and for different heat flux and Reynolds number equals to 724 are shown in **Fig. (4) & Fig. (5)**, respectively. The effect of heat flux and Reynolds number on the inner cylinder temperature variation is the same as that obtained in the horizontal and inclined positions.

The extent of mixed convection depends on the relative magnitude of the heat flux and Reynolds number for the same angle of inclination. When heat flux and Reynolds number are kept constant, the extent of local mixing due to the buoyancy effect in a horizontal annulus is larger than other annulus angle of inclination. It can be expected that for the same condition of flow rate and input heat flux, the inner surface temperature variation along the annulus decreases as the angle of inclination changes from vertical to horizontal position.

Angle of Inclination Effect on the Temperature Distribution

The effect of inclination angle on the inner cylinder temperature variation for q=680 W/m^2 and Re=300 is shown in **Fig. (6)**. Figure shows a reduction in surface temperature as the annulus angle of inclination changes from vertical to horizontal position. This reduction slightly reverses downstream if the angle position changes from 0° (horizontal) to 40° and Reynolds number increases to 724 because of dominant forced convection in the heat transfer process as shown in **Fig. (7)**.

This behavior entirely reverses if the Reynolds number increases to 845 at the same heat flux as shown in **Fig. (8)**. The temperature variation along the surface at the same axial distance is approximately the same for α=70° and 90° (vertical), and slightly decreases upstream and reverses downstream as angle of inclination changes from 0° (horizontal) to 40°. The final behavior can be explained as follows: at annulus entrance, the effect of free convection is small and a predominant forced convection causes the surface temperature of the 70° and 90° (vertical) angle of inclination less than that of 0° (horizontal) and 40° angle of inclination, after a certain axial distance a significant reduction in the inner surface temperature as the inclination angle changes from 0° to 40° due to the free convection begins to dominant flow mixing which reduces the inner surface temperature. This behavior leads to the following conclusion that the heat transfer process improves as the angle of inclination varied from horizontal to vertical when Reynolds number is enough high because of the dominant forced convection in the heat transfer process and vice versa at low Reynolds number case. The increasing of heat flux decreases forced convection effect and the natural convection will be the dominant factor in the heat transfer process.

Local Nusselt Number (Nu_z)

The effect of heat flux on the Nu_z in the horizontal position for Re=218 is shown in **Fig. (9)**. It is clear that the results of higher heat flux for Nu_z were higher than that of lower heat flux. Figure shows also sharp decrease for the local Nusselt number values at the entrance of the annulus then become almost constant downstream for low heat flux (q=96 W/m^2) and increases as heat flux increases. This attributes to increase in both the thermal boundary layer thickness and the surface to bulk air temperature difference which accompany with an increase in the surface heat flux and that accelerate the development of secondary flow downstream.

The effects of Re on Nu_z variation with ZZ is shown in **Fig. (10)** for heat flux equal to 679 W/m^2 : respectively. For constant heat flux, results depicted that the deviation of Nu_z value moves towards the left and increases as the Reynolds number increases. This is obvious from inverse Graetz number (ZZ) which decreases as the Re increases. This situation reveals the domination of forced convection on the heat transfer process with a little effect of buoyancy force at high Re. As the Re reduces the buoyancy effect expected higher which improve the heat transfer process. The minimum value of the Nu_z increases as Re increases then the value of Nu_z increases further downstream for all curves due to strong natural convection in this region.

In horizontal annulus, the effect of the secondary flow is high, hence at low Reynolds number and high heat flux, situation makes the free convection predominant, since as the heat flux increases, the fluid near the heated wall becomes warmer and lighter than the bulk fluid in the annular gap core towards the outer wall. As a sequence, two upward currents for each side of the vertical plane flow along the heated side wall, and by continuity, the fluid near the outer wall of the annulus flow downward. This sets up two longitudinal vortices, which are symmetrical about a vertical plane .

As heat flux further increases the structure of the cellular motion changes from one-cell on each side of the annulus to two and gradually into a multi-cell structure. It is expected that the intensity of vortex increases downstream. The longitudinal vortex (or, in another express, the cellular motion) behaves so as to reduce the temperature difference between the heated inner cylinder surface and the air flow in which led to increasing the growth of the hydrodynamic and thermal boundary layer along the heated cylinder and causes an improvement in the heat transfer coefficient. At low heat flux and high Reynolds number the situation makes forced convection predominant and vortex strength decreases which decrease the temperature difference between the heated surface and the air, hence, the Nu_z values become close to the vertical cylinder values for the same conditions as be seen later.

The variation of the local Nusselt number with ZZ in the vertical position for Re=724 and various heat flux is shown in **Fig.(11)**. Curves depicted have the same general shape shown in **Fig. (9)**. The effect of Re on Nu_z for q=382 W/m^2 and the same position is shown in **Fig. (12)**. Results reveal that the effect of heat flux and Reynolds number on heat transfer coefficient in vertical position gives a similar trend as obtained for horizontal position.

Angle of Inclination Effect on Nu_z

Results for q=680 W/m^2 and Re=300, 724, and 845 are shown in **Fig. (13)**, **Fig. (14)**, and **Fig. (15)**; respectively. It is noticed from the first two figures that at the same axial distance the local Nusselt number value increases as the angle of inclination deviates from the vertical to the horizontal position. As explained before that with the free convection domination, for horizontal position creates upward airflow along the inner heated cylinder surface to form vortices having their center in the annulus upper part with the very complicated flow pattern and with the vortex intensity reduces as the angle of inclination change from horizontal to vertical position leading to increase the extent of the local mixing along the annulus due to high vortices intensity. As a result , the heat transfer process improves as angle of inclination deviates from vertical to horizontal position.

Other reverse situation will be obtained if the Reynolds number increases to 845 at the same heat flux as shown in **Fig. (15)**. For the same ZZ the Nu_z value increases gradually as the inclination

angle deviates from the horizontal to the vertical position. This behavior continues till a certain ZZ value (0.0105) where beyond it the Nu_z value becomes more closer to each other, and gives approximately equal value for each α=[0^o (horizontal) and 40^o] and α=[70^o and 90^o (vertical)].
In general, this situation relates to the small buoyancy effect at annulus entrance and a pure forced convection is dominant heat transfer process. Downstream, the secondary flow becomes more effective which improves the flow mixing and improves the heat transfer process which appears to be higher in the horizontal position and it's effect reduces as the annulus position deviates towards vertical position. As a result, the Nu_z value becomes closer to each other at this region at the same ZZ.
Fig. (16) and **Fig. (17)** show the effect of angle of inclination on the heat transfer processes for q=265 W/m^2, Re=154 and 378; respectively. **Fig. (17)** gives the same behavior that obtained in **Fig. (14)**, but the problem is in **Fig. (16)** which at the early sight may causes a distortion in a physics concepts that concluded from the previous figures of the local Nusselt number. Hence, if the light is perfectly focused on this natural behavior, the problem will be entirely understood. In this figure, in spite of low Reynolds number the local Nusselt number value at the entrance for the same ZZ increases gradually as the inclination angle deviates from the horizontal to the vertical position, then becomes closer to each other in the region bounded between semi-logarithmic value of ZZ=0.1 and 0.109, then a reverse situation occurs further downstream, and the Nu_z value becomes higher as the angle of inclination deviates from the vertical to the horizontal position.
This situation may be expected to occur due to a reverse flow existence at the entrance in $\alpha=40^o$, 70^o , and 90^o (vertical) due to high heat flux relative to Reynolds number creates a distortion in flow pattern and makes the air particals reverse near the heated wall due to very low density if comparison with these in the annular gap. The reverse flow enhance the heat transfer process and gives high Nu_z value. Further downstream the natural convection in horizontal and inclined positions will be stronger in that of vertical position leads to improve of heat transfer process in this positions greater than vertical position.

Correlation of Average Heat Transfer Data

The values of the Nu_m for horizontal ($\alpha=0^o$), inclined ($\alpha=40^o$, 70^o), and vertical ($\alpha=90^o$) positions are plotted in **Figs. (18–21)** in the form of $\log(Nu_m)$ against $\log(Ra/Re)$ for the range of Re from 154 to 845, and Ra from 0.4767×10^5 to 1.3261×10^5 . All the points as can be seen are represented by a straight lines of the following equations:

$\alpha=0^o$ (horizontal) $\quad Nu_m=259.402\,(Ra/Re)^{-0.389}$ (17)

$\alpha=40^o$ $\quad Nu_m=265.199\,(Ra/Re)^{-0.40147}$ (18)

$\alpha=70^o$ $\quad Nu_m=326.960\,(Ra/Re)^{-0.413693}$ (19)

$\alpha=90^o$ (vertical) $\quad Nu_m=476.150\,(Ra/Re)^{-0.50374}$ (20)

It was shown that the heat transfer equations for all the positions have the same following form:

$$Nu_m= a\,(Ra/Re)^d \qquad (21)$$

Where a and d are given in **Table (1)**
The values of d which represent the slope of each curve decrease as the inclination angle deviates from horizontal to vertical position due to decreasing of the buoyancy effect.

The general equation that described the heat transfer process for a selected Re range from 154 to 845 and Ra range from 0.4767×10^5 to 1.3261×10^5 and inclination angle range from 40° to 90° (vertical) was derived in the following form:

$$(Nu_m)_{inc.} = 32.371\ (Ra)^{-0.389}.(Re)^{0.655}.[\sin(\alpha)]^{-2.70108} \qquad (22)$$

The values of measured Nu_m are compared with that of Nu_m calculated from eq.(22) as shown in Fig.22 which are represented by the solid line. The dashed upper and lower lines represent the maximum and minimum acceptable deviation between them which equal to ±15.3 %.

CONCLUSIONS

1- The variation of the surface temperature along the inner cylinder at all angles of inclinations is affected by the extent of the local mixing which increases as the heat flux increases, Re decreases and annulus orientation deviates from vertical to horizontal. The increase of local mixing causes an improvement in the local heat transfer process and reducing the heated surface temperature.

2- The variation of Nu_z with ZZ at any angle of inclination was affected by many variables summarized in the following points:

a- For the same Re and annulus orientation, the Nu_z increases with heat flux.

b- For the same heat flux and annulus orientation, the heat transfer process is dominated by:

i- Forced convection as Re increases and becomes relatively high if comparison with the applied heat flux.

ii- Natural convection as Re decreases and becomes low relatively if comparison with the applied heat flux.

c. For the same heat flux & Re , the Nu_z value decreases as cylinder position changes from horizontal towards vertical (i.e., the minimum value occurs in the vertical position and the maximum value occurs in the horizontal position).

3. The effect of buoyancy is small at the annulus entrance and increases in the flow direction.

REFERENCES

Ciampi, M., Faggiani, S., Grassai, W. and Incropera,F. P., (1986). Experimental study of mixed convection in horizontal annuli for low Reynolds numbers , Proceedings of the 8th Int. Heat Transfer Conference , München, Fed. Rep. of Germany Vol. 3 , pp. 1413-1418,.

Ciampi, M., Faggiani, S., Grassai,W. and Tuoni, G., (1987), Mixed convection heat transfer in horizontal, concentric annuli for transitional flow conditions, Int. J. Heat Mass Transfer, Vol. 30, No. 5, pp. 833-841,.

El-Shaarawi, M. A. I. and Sarhan , (1980), Combined free and forced convection laminar flow in a vertical concentric annuli, J. Heat Transfer , Vol. 102 , pp. 617-622,.

Falah, (1993), Combined free and forced convection in an inclination annulus, Thesis, University of Basra, College of Engineering, Mechanical Department,.

Grimson, J. , (1971), Advance fluid dynamics and heat transfer , Mc Graw-Hill , England ,.

Hanzawa, T. , Sako, A. , Endo, H. , Kagwa, M. , and Koto, K. , (1986), Combined free and forced laminar convective heat transfer from isothermally heated inner tube in vertical concentric annulus, J. Chemical Engineering of Japan ,Vol. 19 ,No. 1, pp. 78- 81 ,.

Hessami, M. A. , De Vahl Davis, G., Leonardi, E. and Reizes, J. A. , (1987), Mixed convection in vertical , cylindrical annuli , Int. J. Heat Mass Transfer , Vol.30, No.1 , pp. 151-164 , January ,.

Kays, W. M., (1966), Convective Heat transfer, Mc Graw-hill , New York,.

Lundberg, R. E. , Reynolds, W. C. and Mc Cuen, P. A. , (1962), Heat transfer in annular passages . General formulation of the problem for arbitrary wall temperature or heat fluxes, Int. J. Heat Mass transfer , Vol.6 , pp. 438-439 ,.

Milano, G. and Guglielmini, G. , (1988), Mixed convection of air in internally heated vertical concentric annuli, Proceedings of the 8th Int. Heat Transfer Conference , München, Fed. Rep. of Germany, Vol.3 , pp. 1041-1056,.

NOMENCLATURE

A : annular gap area; m^2
A_1: inner cylinder surface area; m^2
D_h: hydraulic diameter=$2(r_2-r_1)$: m
I: current; Amp
κ : thermal conductivity; $W/m^2.°C$
L: annulus length; m
$\dot{m}$: volumetric flow rate; m^3/s
$(Nu_m)_{inc.}$: mean Nusselt number at any angle of inclination
Q: convection heat loss; W
Q_t: total heat given; W
Q_{cr}: convection- radiation heat loss; W
q_r: radiation heat flux; $W/m^2.°C$
q: convection heat flux; $W/m^2.°C$
r_1: outer radius of inner cylinder; m
r_2: inner radius of outer cylinder; m
V": voltage; volt

Table (1) Constants in Eq.(21) for Various Angles of Inclination.

α	a	d
0° (horizontal)	259.402	–0.389
40°	265.199	–0.40147
70°	326.96	–0.413693
90° (vertical)	476.15	–0.50374

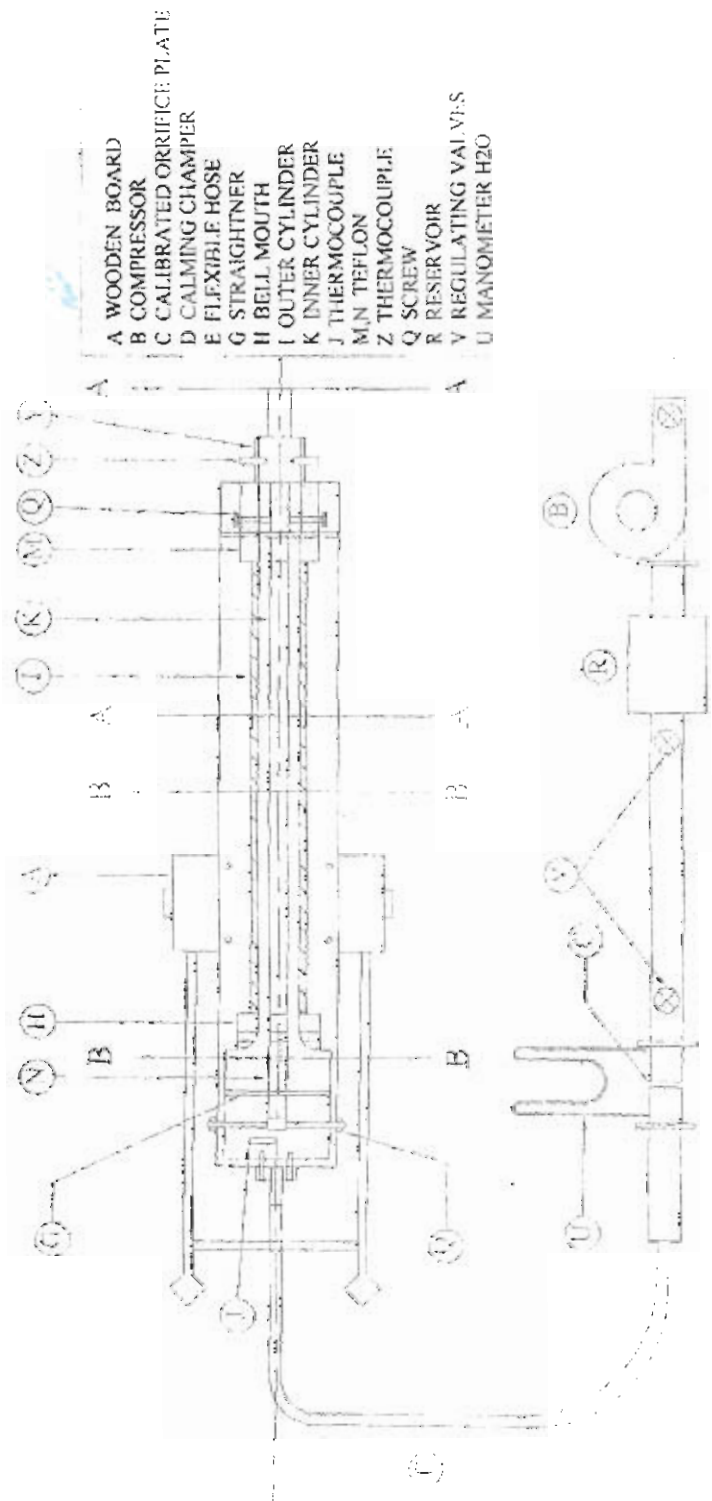

Fig.(1) Diagram of Experimental Apparatus.

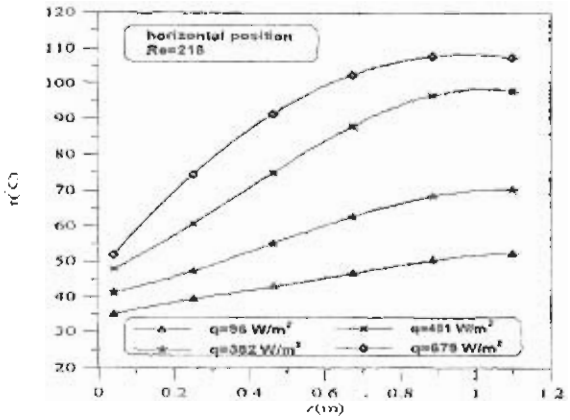

Fig.(2) Variation of the Surface Temperature with the Axial Distance, Re=218, α =0° (Horizontal) .

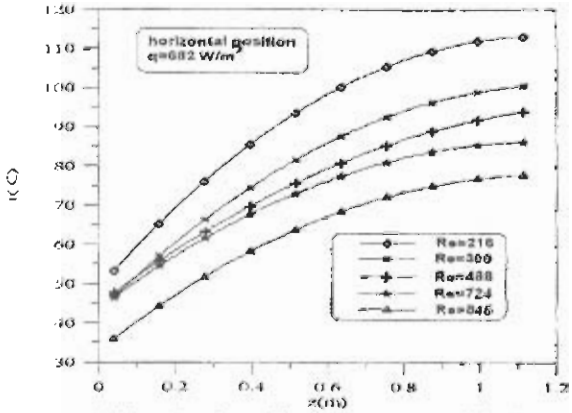

Fig.(3) Variation of the Surface Temperature with the Axial Distance, q=682 W/m^2, α =0° (Horizontal).

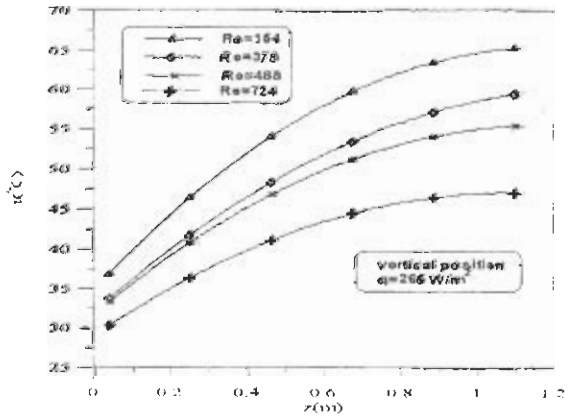

Fig.(4) Variation of the Surface Temperature with the Axial Distance, q=265 W/m^2, α =90° (Vertical).

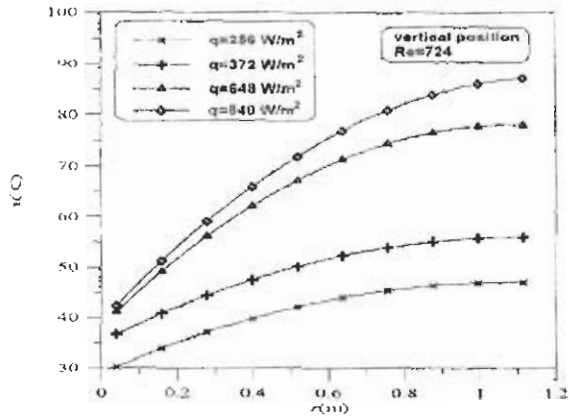

Fig.(5) Variation of the Surface Temperature with the Axial Distance, Re=724, α =90° (Vertical).

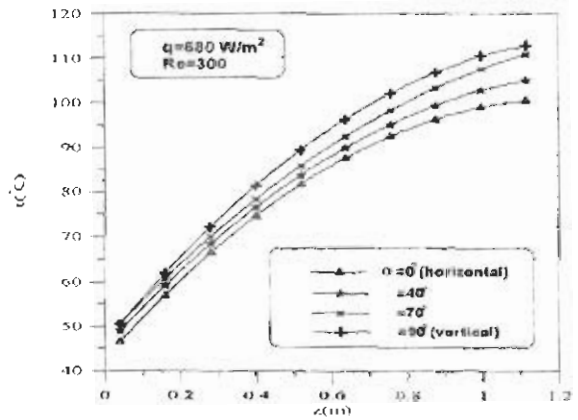

Fig.(6) Variation of the Surface Temperature with the Axial Distance for Various Angles, q=680 W/m^2, Re=300.

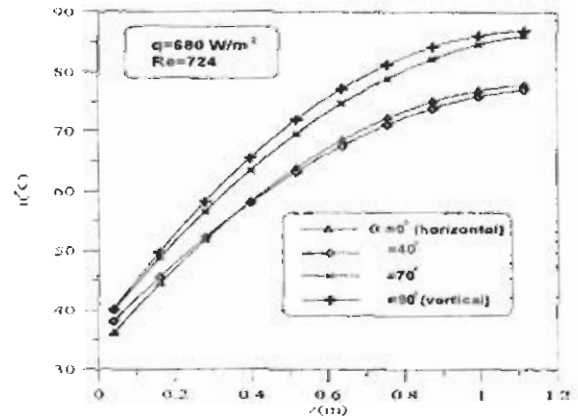

Fig.(7) Variation of the Surface Temperature with the Axial Distance for Various Angles, q=680 W/m^2, Re=724.

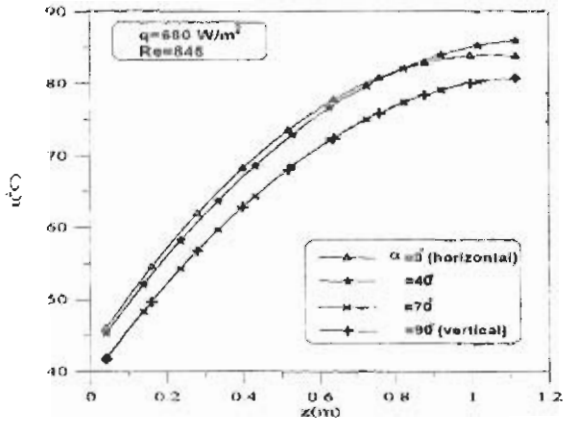

Fig.(8)Variation of the Surface Temperature with the Axial Distance for Various Angles, q=680 W/m^2, Re=845.

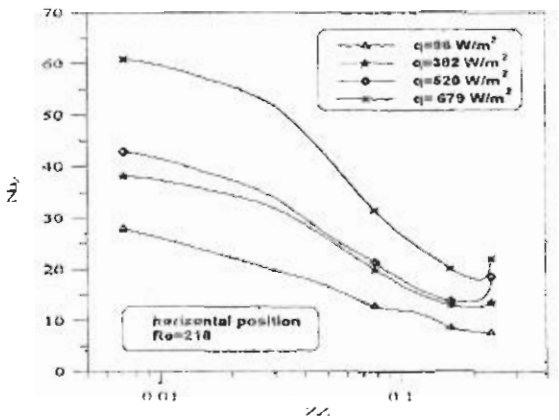

Fig.(9) Local Nusselt Number Versus Dimensionless Axial Distance, Re=218, $\alpha = 0^\circ$ (Horizontal).

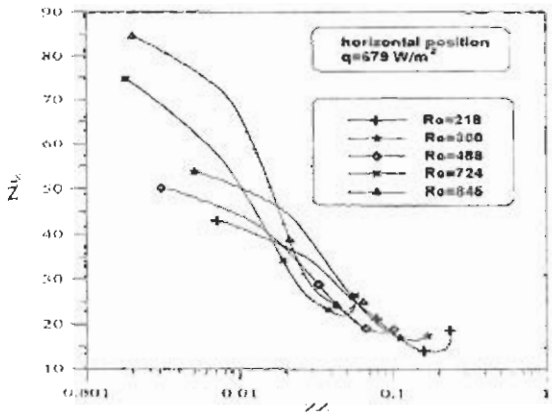

Fig.(10) Local Nusselt Number Versus Dimensionless Axial Distance, q=679 W/m^2, $\alpha = 0^\circ$ (Horizontal).

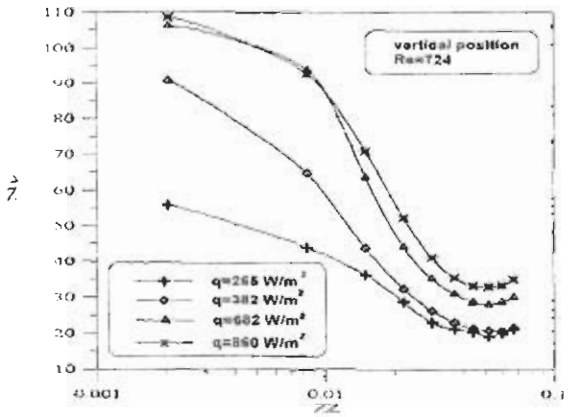

Fig.(11) Local Nusselt Number Versus Dimensionless Axial Distance, Re=724, α =90° (Vertical).

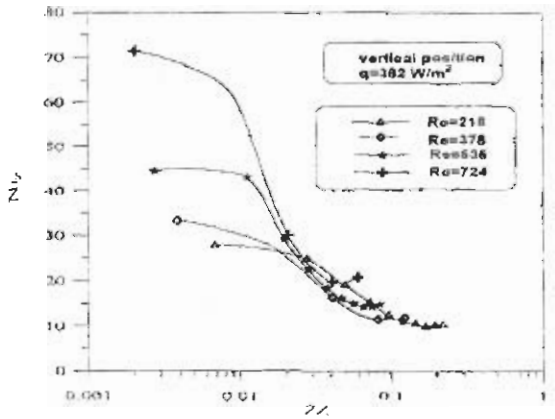

Fig.(12)Local Nusselt Number Versus Dimensionless Axial Distance, q=382 W/m^2, α =90° (Vertical).

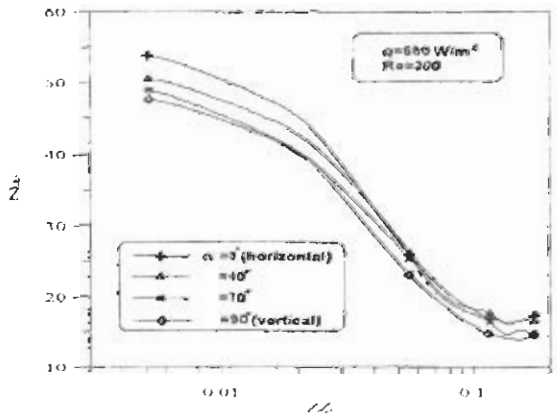

Fig.(13) Local Nusselt Number Versus Dimensionless Axial Distance for Various Angles, q=680 W/m^2, Re=300.

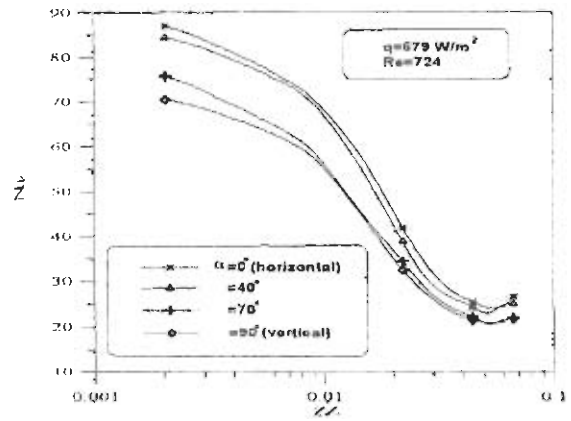

Fig.(14) Local Nusselt Number Versus Dimensionless Axial Distance for Various Angles, q=679 W/m^2, Re=724.

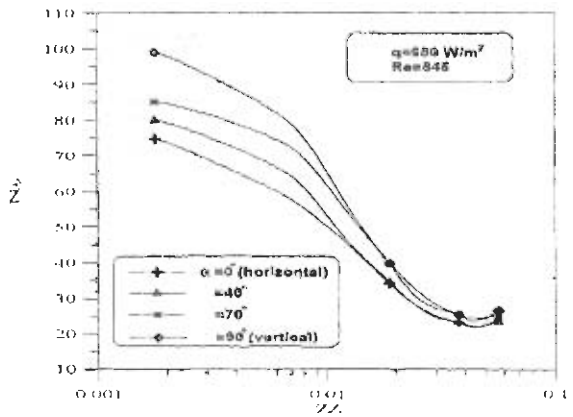

Fig.(15) Local Nusselt Number Versus Dimensionless Axial Distance for Various Angles, q=680 W/m^2, Re=845.

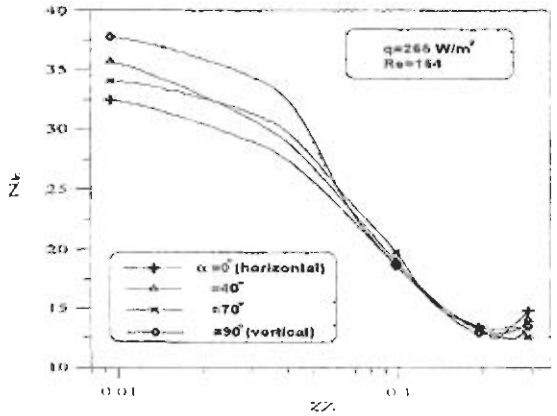

Fig.(16) Local Nusselt Number Versus Dimensionless Axial Distance for Various Angles, q=265 W/m^2, Re=154.

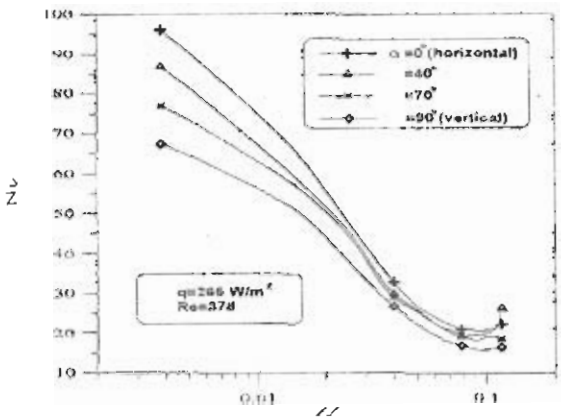

F ig.(17) Local Nusselt Number Versus Dimensionless Axial Distance for Various Angles, q=265 W/m^2, Re=378.

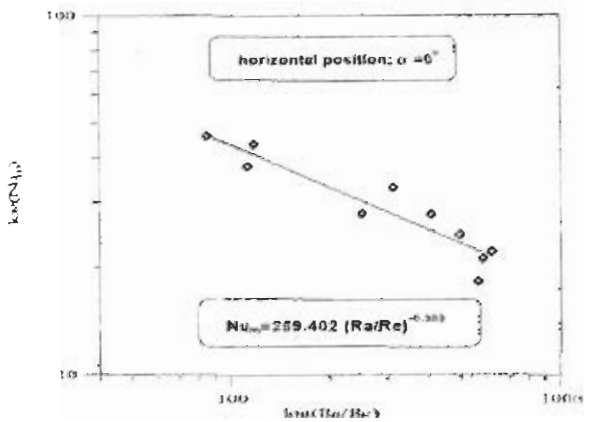

Fig.(18) Logarithm Average Nusselt Number Versus log(Ra/Re), $\alpha = 0^{\circ}$ (Horizontal).

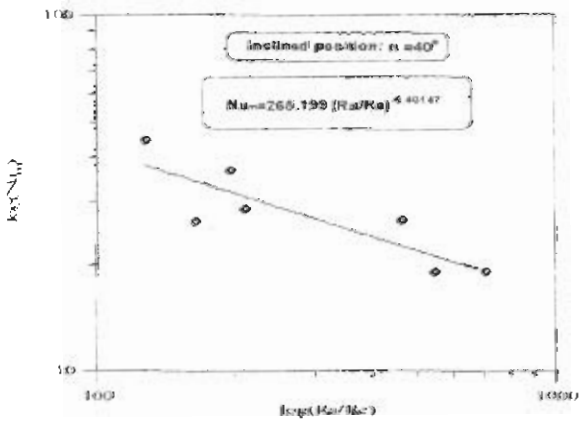

Fig.(19) Logarithm Average Nusselt Number Versus log(Ra/Re), $\alpha = 40^{\circ}$.

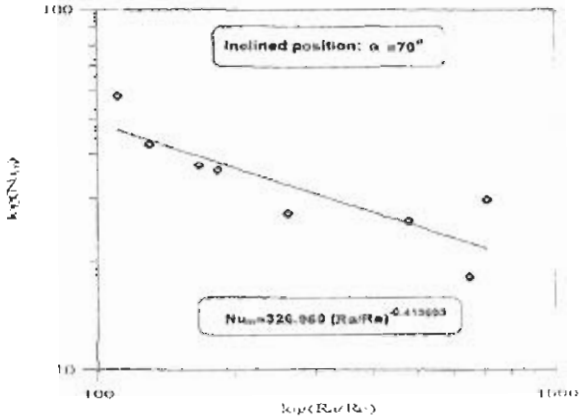

Fig.(20) Logarithm Average Nusselt Number Versus log(Ra/Re), $\alpha = 70^{o}$.

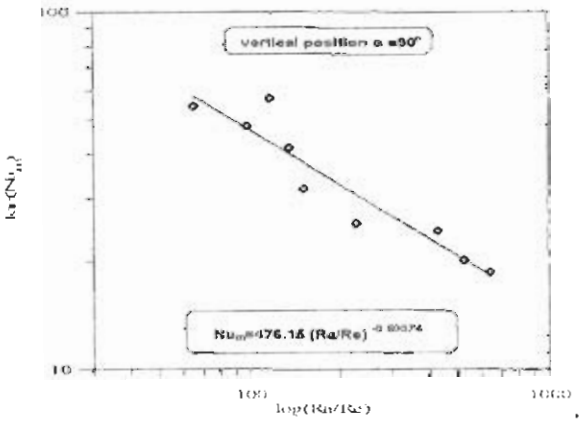

Fig.(21) Logarithm Average Nusselt Number Versus log(Ra/Re), $\alpha = 0^{o}$ (Vertical).

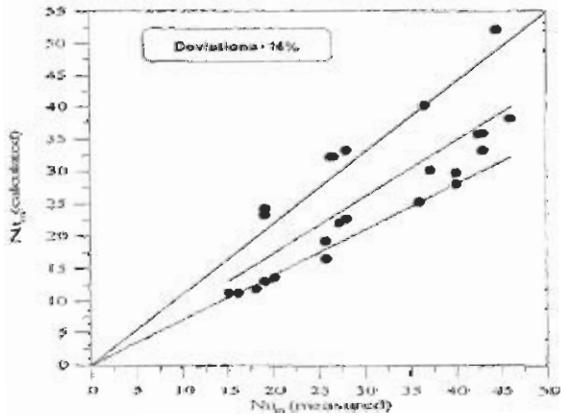

Fig.(24) Comparison Between Measured Nu_m and Nu_m Calculated from eq.(22).